Applied Energy 99 (2012) 154–166

Contents lists available at SciVerse ScienceDirect

Applied Energy

journal homepage: www.elsevier.com/locate/apenergy

Wind speed and wind energy forecast through Kalman filtering of Numerical Weather Prediction model output

Federico Cassola [a], Massimiliano Burlando [b,*]

[a] Department of Physics, University of Genoa, Via Dodecaneso 33, 16146 Genoa, Italy
[b] Department of Civil, Environmental, and Architectural Engineering, University of Genoa, Via Montallegro 1, 16145 Genoa, Italy

HIGHLIGHTS

- NWP models are unable to provide reliable wind speed forecast in complex terrain.
- Kalman filtering techniques are widely used to improve the prediction of NWP models.
- Kalman filter is tuned to find the most suitable configuration to predict wind speed.
- The filter is applied to forecast wind speed and wind power at a wind farm site.
- Simulations, corrected by Kalman filtering, show very low errors wrt measurements.

ARTICLE INFO

Article history:
Received 17 November 2011
Received in revised form 9 February 2012
Accepted 26 March 2012
Available online 6 June 2012

Keywords:
Wind speed nowcasting
Short-term wind energy forecast
NWP models performance
Kalman filter
Ligurian wind climate

ABSTRACT

Despite the major progress made by Numerical Weather Prediction (NWP) in the last decades, meteorological models are usually unable to provide reliable surface wind speed forecasts, especially in complex topography regions, because of shortcomings in horizontal resolution, physical parameterisations, initial and boundary conditions. In order to reduce these drawbacks, one of the most successful approaches is the Kalman filtering technique, which combines recursively observations and model forecasts to minimise the corresponding biases. In meteorology, Kalman filters are widely used to improve the prediction of variables characterised by well-defined cyclicities, whereas the evolution of wind speed is usually too irregular. In the present paper, the Kalman filter is analysed in order to find the best configuration for wind speed and wind power forecast. The procedure has been tested, in a hindcast mode, with 2-year-long data sets of wind speed provided by a NWP model and two anemometric stations located in the eastern Liguria (Italy). It is shown that, tuning time step and forecast horizon of the filter, this methodology is capable to provide significant forecast improvement with respect to the wind speed model direct output, especially when used for very short-term forecast. In this configuration, Kalman-filtered wind speed data have been used to forecast the wind energy output of the nearby wind farm of Varese Ligure. After 2 years of testing, the percentage error between simulated and measured wind energy values was still very low and showed a stable evolution.

1. Introduction

Wind energy is nowadays the most important source of renewable energy worldwide. Its very fast rate of growth implies for the electrical systems to be able to absorb large amounts of wind power and deliver it on the market. However, due to its stochastic nature, wind energy is not a controllable energy resource that can be scheduled and planned in the same manner as conventional fossil energies, and the cumulative energy input of several wind power plants into the electric grid may cause dangerous fluctuations in the power system. Therefore, reliable wind power prediction systems are required for time scales from minutes to weeks, i.e. for the optimisation of the produced electricity with respect to market requirements (unit commitment, economic dispatch, participation in the electricity markets, etc.), as well as the corresponding uncertainty information for optimising decision-making processes resulting from the use of predictions.

A comprehensive overview of the problem of wind power forecasting is given by Giebel et al. [1]. In general, short-term wind power predictions can be obtained following two different approaches: pure statistical techniques, like Kalman filtering [2,3], auto-regressive and fuzzy logic models [4,5], artificial neural

* Corresponding author. Tel.: +39 010 353 2509; fax: +39 010 353 2534.
E-mail addresses: cassola@fisica.unige.it (F. Cassola), massimiliano.burlando@unige.it (M. Burlando).

0306-2619/$ - see front matter © 2012 Elsevier Ltd. All rights reserved.
http://dx.doi.org/10.1016/j.apenergy.2012.03.054

networks [6–8], etc., try to find the relationships between some explanatory variables and online measured power data (for instance from the Supervisory Control And Data Acquisition system of a wind turbine); physical approaches use mainly physical considerations, like Numerical Weather Prediction (NWP) model results, to obtain an estimate of the local wind speed forecast. Typically, prediction models using NWP forecasts outperform statistical approaches after 3–6 h look-ahead time, whereas statistical approaches turn out to be quite reliable for very short-term forecasts, i.e. less than 6 h. The optimal model probably consists in a mixed approach, which is very often adopted by utilities in order to combine high accuracy for very short horizons together with longer forecasts up to 48–72 h. In the present paper, we focus on a mixed approach based on the use of a NWP model coupled to a statistical model based on the Kalman filtering technique.

Numerical Weather Prediction models are general-purpose models as, in principle, they can be used for whatever problem concerning atmospheric physics including wind power meteorology. They are not specific, however, for wind energy applications and the maximum resolution they can reach is of the order of two kilometres in their non-hydrostatic version, while for wind energy applications, and micrositing in particular, higher resolutions are usually required. Besides, it is well known that NWP models often exhibit systematic errors in the forecast of certain meteorological parameters, like wind speed and direction, especially near the surface [9,10] and onshore, where one of the main sources of error is just the model horizontal resolution, since the associated smoothing and averaging of the orographic and landscape characteristics lead to a weak representation of the local effects on the airflow. Increasing the model resolution may provide considerable improvement in the representation of smaller-scale flow characteristics. Nevertheless, an open question remains as to whether the use of higher-resolution limited-area models improves the forecast skill considerably. Even if this were true, it is still uncertain whether such improvement compensates for the usage of increasing computational resources required for these applications [11]. Further contributions to the forecast error are in fact typically given by the shortcomings in the physical parameterisations and the subsequent inability by NWP models to successfully handle subgrid-scale phenomena, as well as by interpolations to areas that are not close to model levels. In addition to these model-related issues, inaccuracies in the NWP model forecasts may also be due to possible errors in the initial and lateral boundary conditions driving the simulations. Finally, it is worth noting that an error on the wind flow prediction by the NWP model becomes three times larger when wind speed is converted into wind power, so that using NWP models for wind energy purposes is even more critical than for other applications.

In order to reduce the influence of the abovementioned drawbacks in the final output of a NWP model, a variety of approaches based on statistical methods have been used. Most of them are derived from Model Output Statistics (MOSs), which are able to account for local effects and seasonal changes. MOS uses multiple linear regression to produce an improved forecast at specific locations by using model forecast variables and prior observations as predictors [12,13]. MOS remains a useful tool and during the 2002 Olympic Winter Games, MM5-based MOS outperformed the native forecasts produced by MM5 and was equally or more skilful than human-generated forecasts by the Olympic Forecast Team [14]. However, discrepancies have been found in MOS applications in cases of short-time local weather changes or updates of the atmospheric model in use (see e.g. [15–17]).

One of the most successful approaches to this problem is the use of Kalman filters (see references in Section 3). They consist of a set of mathematical equations that provides an efficient computational solution of the least-square method. In practice, the Kalman filter is the statistically optimal sequential estimation procedure for dynamic systems. Observations are recursively combined with recent forecasts using weights that minimise the corresponding biases. The main advantage of this statistical methodology with respect to MOS is the easy adaptation to any alteration of the observations as well as the fact that it may utilise short series of background information. The recursive nature is one of the very appealing features of the Kalman filter and makes practical implementations much more feasible than, for instance, an implementation of a Wiener filter [18], which is designed to operate on all of the data directly for each estimate. The Kalman filter, instead, conditions recursively and implicitly the current estimate on all of the past measurements.

As far as meteorological applications are concerned, Kalman filters are widely used both in data assimilation and improving weather forecasts [2,17,19–27]. In particular, the application of Kalman filters has been proven to give encouraging results for both temperature and wind speed prediction, with a significant reduction of systematic errors [17,23–25]. Some specific attempts to apply this technique to wind power prediction have been recently made as well (c.f. ANEMOS project[1]; [24,28]).

In this paper, the application of Kalman filters to locally adjust the low-resolution numerical prediction of the wind speed and wind power production of a NWP model at the wind farm site of Varese Ligure (Northern Italy) is shown. The aim of this procedure is to test whether the wind speed predicted by a NWP model, V_i^{NWP}, and corrected by ΔV_i through a Kalman filter with the local measurements at a set of sites of coordinates $\{(x_i, y_i)$ with $i = 1,\ldots,I\}$ can be used to predict the wind speed at other sites of coordinates $\{(x_j, y_j)$ with $j = I+1,\ldots,J\}$. In particular, the corrections ΔV_i obtained at sites (x_i, y_i) where measurements are available, are interpolated in order to estimate the corresponding corrections ΔV_j at sites (x_j, y_j) where the wind speed $V_j = V_j^{NWP} + \Delta V_j$, and possibly the energy production, is required. The present test is based on the simulations of the NWP model BOLAM, two anemometric measurement masts of coordinates (x_i, y_i) at Casoni di Suvero and Lago di Giacopiane, not far from the wind farm of Varese Ligure, and the wind speed and energy production data at the wind farm site of coordinates (x_j, y_j). Wind speed and energy production data of the wind farm of Varese Ligure have been used to test the performance of the whole procedure. It is worth noting that this procedure could be used for the short-term forecast of the energy production of a wind farm as well as to assess the wind resources of a site where direct measurements are not available but anemometric stations close to the site exist.

Some testing to the Kalman filtering technique has been carried out as well, in order to find the filter configuration which performs best: filtering has been applied at different forecast horizons depending on the criteria adopted in the update process and, in addition to the classical linear algorithm, the implementation of non-linear polynomial functions in the filter, as proposed by Galanis et al. [23], has been considered. Kalman-adjusted wind speeds have been statistically compared with the observations of the two anemometric masts of Casoni di Suvero and Lago di Giacopiane to test the performance of the different configurations.

The available numerical simulations and anemometric measurements, and the wind farm of Varese Ligure are described in Section 2. A brief general introduction to Kalman filters and the specific methodology followed in the present work is illustrated in Section 3. Results concerning the optimisation of the Kalman filter for wind speed prediction and the application of Kalman filtering for wind power prediction are presented and discussed in Sections 4 and 5, respectively. Finally, conclusions are drawn in Section 6.

[1] http://anemos.cma.fr; http://forecast.uoa.gr/anemos/.

2. Numerical simulations, wind speed and energy production data sets

In the present study, three kinds of different data have been used: wind speed data simulated by means of a NWP model; wind speed data measured at two anemometric masts (Casoni di Suvero and Lago di Giacopiane), used for the correction of the previous simulation through Kalman filtering; wind speed and energy production data of a wind farm (Varese Ligure), used to test the Kalman filtering correction and to check whether the quality of the correction is high enough for wind energy purposes. In the following subsections, the aforementioned three kinds of data are briefly described.

2.1. The NWP model BOLAM

The proposed methodology has been applied to improve locally the wind speed forecasts provided by the BOLAM model, developed at the Institute of Sciences of Atmosphere and Climate (ISAC) of the National Research Council (CNR) in Bologna, Italy [29,30]. It is a finite-difference, primitive-equation, hydrostatic, limited-area NWP model and is used operationally at the Meteo-Hydrological Center of Liguria Region (CFMI-PC) and at the Oceanic and Atmospheric Physics Group at the Department of Physics (DIFI) of the University of Genoa, Italy, thanks to a special agreement between these three institutions. It is also used at the National Observatory of Athens (Greece) [31] and at the Agrometeorological Service of Sardinia Region (Italy).

BOLAM is a grid-point hydrostatic model in sigma coordinates, with variable spacing in the vertical such as to give higher resolution near the surface and, to a smaller extent, near the tropopause. Horizontal discretisation for the enstrophy- and energy-conserving second-order advection scheme is performed on an Arakawa C-grid. The prognostic variables are: zonal (u) and meridional (v) wind components, potential temperature (θ), specific humidity (q), and surface pressure (p_s). The physical package includes vertical diffusion, dry adiabatic adjustment, soil water and energy balance, radiation, large-scale precipitation and evaporation, and parameterisation of moist convection. In particular, as far as the parameterisation of the boundary layer is concerned, vertical diffusion, confined to the lower part of the troposphere, is a parameterisation of turbulent mixing of momentum, potential temperature and specific humidity. The scheme is based on a mixing-length hypothesis, with exchange coefficients depending on the Richardson number. Bottom boundary fluxes of the above quantities are a linear function of the wind speed at the lowest sigma level and of the vertical gradient of the quantity in the layer between the lowest sigma level and the ground. The constant of proportionality depends on the Richardson number in such layer above the ground and on surface roughness.

BOLAM model has been validated especially concerning its skill in predicting precipitation rates and surface fields in case of orographic cyclogenesis and extreme events [29,31–35]. The model has been also tested within the framework of a research focused on the intercomparison of four different mesoscale meteorological models for precipitation forecasting [36]. Yet, it is run in ensemble configuration at the National Observatory of Athens [37].

Since June 2003 several versions of BOLAM with different spatial horizontal resolution have been running daily at DIFI. For the present study, the highest-resolution version of the model (BOLAM 7) has been used, centred over Northern Italy with a horizontal grid spacing of about 7 km. Initial and boundary conditions are provided by a coarser version of the model (BOLAM 21), covering Northern and Central Europe and the Northern Coast of Africa with a spatial resolution of 21 km. Fig. 1 shows, in the left panel, the computational domain of BOLAM 7.

Forecasts are archived every 3 h and the run length is 42 h, starting every day from 06 UTC. The NCEP global model GFS gridded fields at the horizontal resolution of one degree drive BOLAM 21 simulations.

2.2. The anemometric data sets of Casoni di Suvero and Lago di Giacopiane

The observational database consists in wind speed recordings at 10 m AGL from two anemometric stations belonging to the Meteo-Hydrological Observatory of Liguria Region (OMIRL), managed by the Regional Agency for Environmental Protection (ARPAL). Measurements are averages over 10 min, and the sampling rate is also 10 min. Every data set used in the present study is 2-year long, namely from 1 January 2007 to 31 December 2008.

In Columns 2–4 of Table 1 the geographical coordinates and the elevation of each considered station are reported, while in Fig. 1 (right panel) an image of the Ligurian territory highlighting the position of the two stations (circles) is presented. The two stations are located at rather high altitudes, in a typical inland environment. In Fig. 2, the wind roses for each station, divided into 7 speed classes and 16 sectors of 22.5° amplitude each, are presented. It is worth noting that the two stations, despite the complexity of the Ligurian territory, are located in areas with very similar sheltering and channelling effects, as pointed out by the shape of the observed statistical distributions of wind speed and direction. Casoni di Suvero, however, is characterised by higher wind speeds than Lago di Giacopiane, as shown in Column 5 of Table 1, which reports the average wind speed values calculated in the considered period of 2 years. This is probably due to the fact that the station Casoni di Suvero is placed on top of the main ridge of the Apennines while the station Lago di Giacopiane is in the highest part of a valley, where speed-up effects are less important.

2.3. Data sets of wind speed and energy production of the wind farm of Varese Ligure

Since 2000, at the site Passo della Cappelletta (squared symbol in Fig. 2), close to Varese Ligure at a height of a bit less than 1100 m ASL, a wind farm has been producing renewable energy. The wind farm consists of four wind turbines for a total nominal power of 3.2 MW, namely two NEG MICON 750/48 installed in 2000 and two Vestas V52 installed in 2005. All the turbines have a hub height of 50 m AGL.

The database used in the present study consists of daily-averaged wind speed and energy production data of the two NEG MICON 750/48 wind turbines for the period from 1 January 2007 to

Table 1
Geographical and anemological information about the considered anemometric stations and the wind turbines of the wind farm at Varese Ligure.

Station	Latitude (°)	Longitude (°)	Elevation (m) ASL	Height (m) AGL	Average speed (m/s)
Lago di Giacopiane	44.461	9.388	1030	10	3.5
Casoni di Suvero	44.305	9.766	1070	10	5.3
NEG MICON 1	44.402	9.662	1076	50	6.4
NEG MICON 2	44.401	9.663	1077	50	7.1

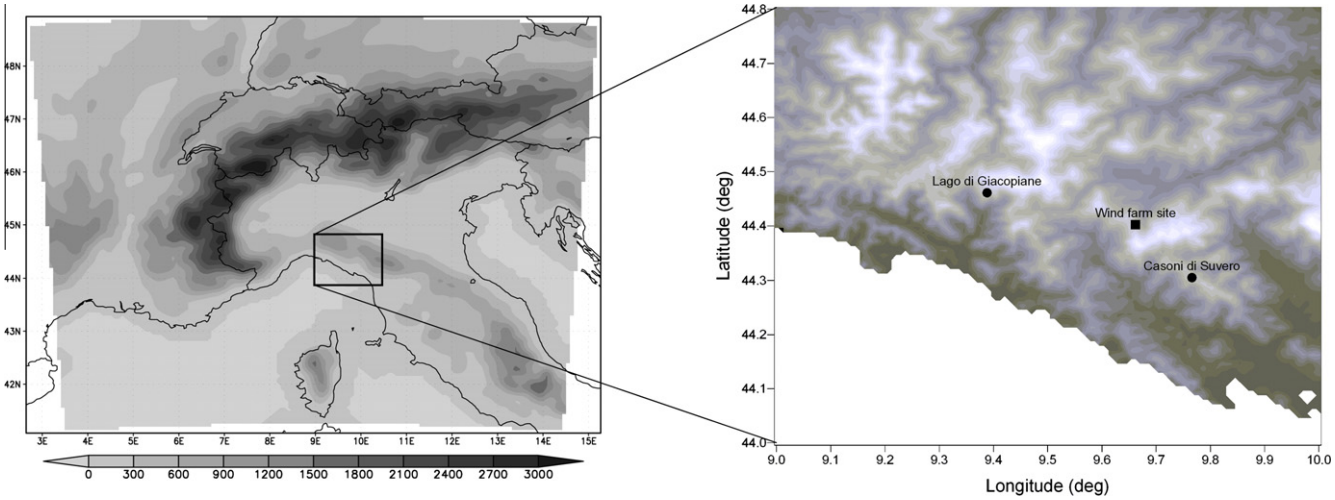

Fig. 1. Left panel: topography of the Northern Italy corresponding to the computational domain of BOLAM 7. Right panel: portion of the Liguria Region where the two anemometric stations Lago di Giacopiane and Casoni di Suvero (circles) and the wind farm of Varese Ligure (square) are located.

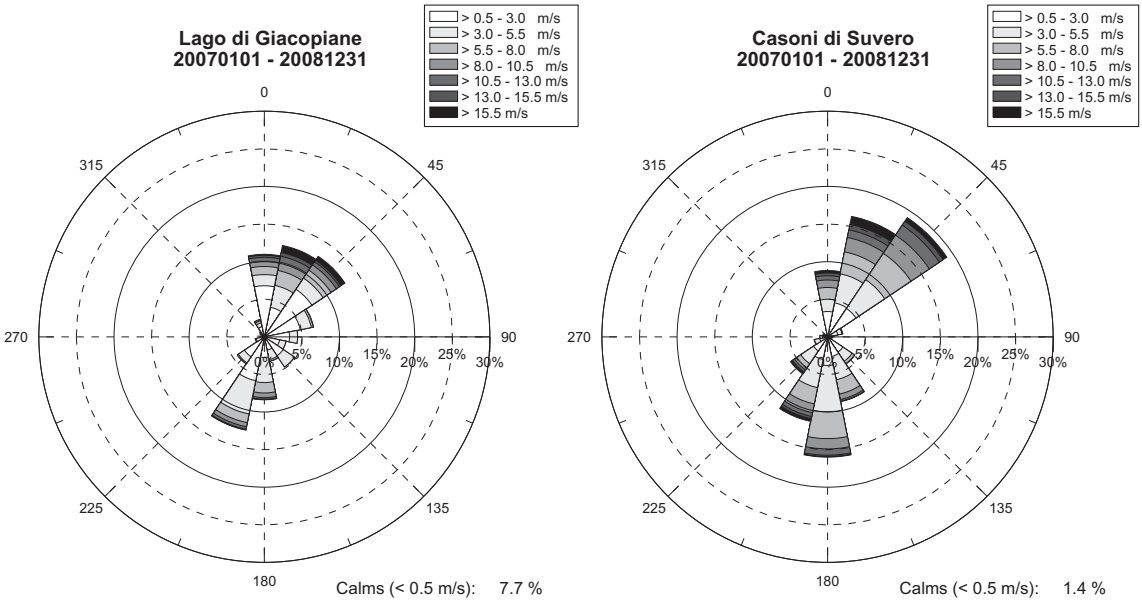

Fig. 2. Statistical distribution of wind intensity and direction of the two anemometric stations Lago di Giacopiane (left) and Casoni di Suvero (right).

31 December 2008. The coordinates of the two wind turbines and the mean wind speed measured at the hub height by the anemometers installed on the nacelle are reported in Table 1.

3. Overview of the Kalman filter

In 1960, Kalman published his famous paper describing a recursive solution to the discrete-data linear filtering problem [38]. Since that time, due in large part to advances in digital computing, the Kalman filter has been the subject of extensive research and application, particularly in the area of autonomous or assisted navigation [18,39–43].

The Kalman filter is an algorithm that provides an efficient computational (recursive) mean to estimate the state of a process, in a way that minimises the mean of the square error. The filter is very powerful in several aspects: it supports estimations of past, present, and even future states, and it can do so even when the precise nature of the modelled system is unknown.

The main goal is the simulation of the evolution in time of an unknown process (state vector), whose value at time t is denoted here by $\mathbf{x}_t$. The Kalman filter provides a method for the recursive estimation of the unknown state based on all observation values up to time t. As such, the equations for the Kalman filter fall into two groups: "time update" equations and "measurement update" equations. The former are responsible for projecting forward (in time) the current state and error covariance estimates to obtain the *a priori* (forecast) estimates for the next time step, while the latter are responsible for the feedback, i.e. for incorporating a new measurement into the *a priori* estimate to obtain an improved *a posteriori* (analysis) estimate.

3.1. Kalman filtering for wind speed prediction

During the last years, Kalman filters have been extensively used for meteorological purposes, both in data assimilation and improving weather forecasts. However, the linear form of the algorithm as

well as the special type (non continuous in some cases) of wind speed time series may constitute, in principle, important drawbacks for such applications on the prediction of wind parameters, affecting significantly the final outcome. Therefore, while the application of classical linear Kalman filters for the improvement of local air temperature predictions seems, in most cases, to be successful [19,20], analogous work for wind speed predictions may lead to poor results [2,45,46].

The proposed approach is based on the correction of the 10-m wind speed forecast bias using a "polynomial" Kalman filter. In particular, the estimation of such bias in time is performed as a function of the forecasting model direct output.

3.1.1. Structure of the filter

Following Galanis et al. [23], let m_t be denoting the direct output of the model at time t at a certain location and z_t the bias of this forecast, defined as $z_t = m_t - o_t$, where o_t is the observed wind speed at the same time. The forecast bias z_t can then be represented by means of m_t as a polynomial function:

$$z_t = a_{0,t} + a_{1,t}m_t + a_{2,t}m_t^2 + \cdots + a_{n,t}m_t^n + v_t \quad (1)$$

where the coefficients $(a_{j,t}), j = 0, 1, \ldots, n$ are the parameters that have to be estimated by the filter and v_t the Gaussian, random, error of the previous procedure. Note that z_t and v_t are scalar variables here, differently from the general case where they are vectors.

Therefore, the state vector is the one formed by the coefficients $(a_{j,t})$, namely:

$$\mathbf{x}_t = [a_{0,t}, a_{1,t}, a_{2,t}, \cdots, a_{n,t}]^T \quad (2)$$

while as system matrix we assume the identity matrix with dimension equal to the order of the filter in use, that is

$$\mathbf{I}_n = \begin{pmatrix} 1 & \cdots & 0 \\ \vdots & \ddots & \vdots \\ 0 & \cdots & 1 \end{pmatrix}$$

The observation procedure is the forecast bias z_t and the observation matrix takes the form:

$$\mathbf{H}_t = [1, m_t, m_t^2, \cdots, m_t^n]^T \quad (3)$$

This kind of methodology allows the implementation of non-linear functions in the Kalman algorithm. The estimation may be of a linear form by choosing as order $n = 1$ in Eq. (1), or a polynomial one of arbitrary degree. It is worth noting that one may employ a polynomial function of arbitrary order. However, on the one hand a plain first-order form might lead to difficulties in the simulation of non-linear procedures, as the wind speed evolution, on the other hand higher-order polynomials result in increased "noise" due to instabilities with no essential contribution in filter accuracy, and hence model output improvement. A detailed study for the determination of the optimum order for a filter polynomial has been investigated in [23], where a low-order polynomial proved to have the best contribution in the elimination of the systematic part of the bias with less need in CPU time. Therefore, in the present work, Kalman filtering of numerically predicted wind speed has been performed adopting a similar approach, choosing a limited range of values for the n parameter, namely $n = 1,2,3,4$.

The initial values for the filtering procedure were also chosen following Galanis et al. [23], in such a way that quick independence from initial conditions and fast adaptability of the filter to any new condition is ensured.

3.1.2. The role of the time step

One of the most critical points when implementing the filter concerns the "time step" τ, that is the interval with which observations are combined with model simulations. A typical choice is to select a forecast horizon (e.g. +6 h, +12 h, +24 h and so on) or, equivalently, a forecast valid time (00 UTC, 06 UTC, 12 UTC, etc.) and to perform Kalman filtering for each particular horizon or valid time. Suppose, for instance, that the model is run once a day, with a run length of 24 h starting at 12 UTC, and that our goal is to adjust the model forecast valid at 00 UTC, corresponding to a forecast horizon of +12 h (Fig. 3). Thus, the filter determines the weights to be applied to the model output every 24 h ($\tau = 24$ h) by evaluating the forecast bias at 00 UTC on the previous days.

This procedure is, in fact, more suitable to describe variables that are characterised by a well-defined diurnal cycle, such as surface air temperature. In this case, the inter-daily variability is quite limited while the correspondence between the temperature readings on subsequent days is strong, thus assuring a good performance of the filter. The evolution of wind speed is, on the contrary, much more irregular and complicated and measurements at a given time are poorly correlated with measurements at the same time on the previous days. Nevertheless, the application of Kalman filters of the above type to different forecasting models and locations has been proven to give encouraging results both for surface air temperature and wind speed, with a significant reduction of systematic errors [2,17,23,24].

In the present study, a twofold approach has been adopted: as a first step, the methodology described insofar has been applied with the aim of improving the wind speed forecast at short to medium range (up to 36 h ahead). The estimation of the process noise covariance $\mathbf{Q}_t$ and the measurement noise covariance R_t is based on the sample of the last seven values of $\mathbf{w}_t = \mathbf{x}_t - \mathbf{x}_{t-1}$ and $v_t = z_t - \mathbf{H}_t\mathbf{x}_t$, respectively:

$$\mathbf{Q}_t = \frac{1}{6}\sum_{i=0}^{6}\left(\mathbf{w}_{t-i} - \frac{1}{7}\sum_{j=0}^{6}\mathbf{w}_{t-j}\right)^2 \quad (4)$$

$$\mathrm{R}_t = \frac{1}{6}\sum_{i=0}^{6}\left(v_{t-i} - \frac{1}{7}\sum_{j=0}^{6}v_{t-j}\right)^2 \quad (5)$$

The latter are objective estimators of $\mathbf{Q}_t$ and R_t since the variables $\mathbf{w}_t$ and v_t, denoting the non-systematic part of errors, follow the normal distribution by assumption. This time period of 7 days was proven to be an adequate choice in order to achieve successful corrections and fast adaptability simultaneously and, at the same time, does not create needs for extended data storage (see [23,24]).

Then, a Kalman filter of the same type but with a different time step τ has been implemented (Section 4.2), with specific nowcasting (6 h maximum) purposes. In particular, the calculation of the covariances $\mathbf{Q}_t$ and R_t is now performed taking into account the last seven predicted and observed values again (Eqs. (4) and (5)), but the time interval is equal to the maximum frequency at which measurements and forecasts are available (3 h in our case). In practice, model predictions and observations are treated as two continuous time series, regardless of the forecast horizon, with a sampling rate every 3 h. It is clear that, in this case, only a very short term correction is reasonable, because the coefficients to be applied to the model output are evaluated on the basis of the recent evolution of predicted and observed wind speeds, so that a longer forward projection of the current state estimated by the filter would lead to poor results. Finally, it is worth noting that, while in the former implementation the Kalman filtering is applied only once a new run of the model gets ready, in the latter the calculation can be updated whenever a new measurement is made available, with the noticeable advantage of providing corrected forecasts at the same sampling rate as the observations at a very low computational cost.

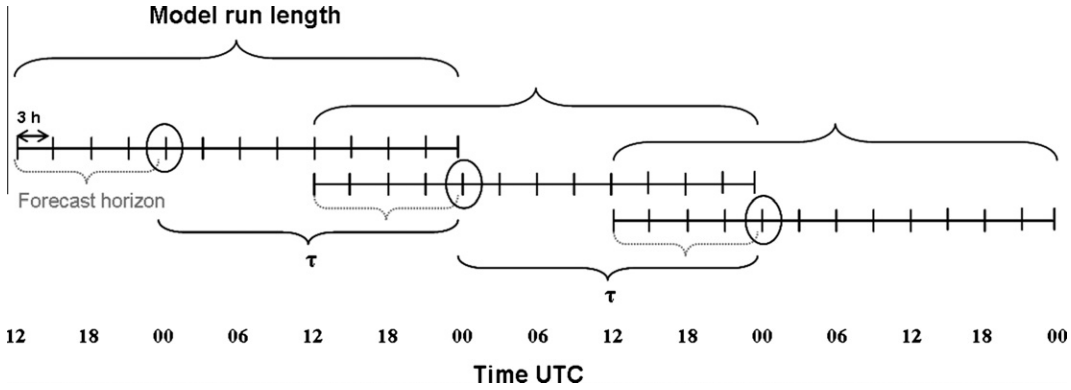

Fig. 3. Schematisation of the Kalman filtering procedure. Model outputs valid at 00 UTC (corresponding to a forecast horizon of +12 h), marked by circles, are adjusted by comparing forecasts and observations at the same time on the previous days (τ = 24 h).

4. Optimisation of the Kalman filter for wind speed prediction

The results presented here are based on a detailed statistical analysis of Kalman-filtered wind speed values with respect to BOLAM direct outputs and observed data. Kalman filtering has been applied in a hindcast mode to the whole 2-year-long data sets. BOLAM gridded fields have been bilinearly interpolated to the exact locations of the anemometric stations Lago di Giacopiane and Casoni di Suvero, taking into account the four grid points closest to each station. Since BOLAM outputs are available every 3 h, while data are recorded every 10 min, only measurements concurrent to the simulation output have been considered.

The assessment of the proposed methodology is based on some classical verification indices (see, for instance, Wilks [47]) as well as the analysis of scatter plots and temporal evolution of predicted and observed values. Concerning the indices, in particular, the mean error (ME), is a crucial parameter for Kalman filtering since any type of Kalman method aims at considerably reducing the systematic part of the forecast error. The success on this issue is the main criterion ensuring the credibility of the filter. This is not contradictory with the fact that the Kalman filter is a minimum mean-square error estimator. The algorithm, indeed, minimises the mean square error in the estimation of the state vector, corresponding to the coefficients to be applied to the model direct output (see Section 3). To evaluate the effectiveness of such estimation, one is interested in assessing the reduction of the systematic error in the wind speed prediction, hence the plain mean error is an appropriate tool. The mean absolute error (MAE) in turn assesses the "real" improvement in the model predictions despite any possible changes in the type of errors. Finally, the Pearson correlation coefficient (r) is a good measure of linear association or phase error. Visually, the correlation measures how close the points of a scatter plot are to a straight line. It does not take forecast bias into account, so that it is possible for a forecast with large errors to still have a good correlation coefficient with the observations.

In the following two subsections the results obtained with the two different Kalman filter implementations described in Section 3.1.2 are illustrated and discussed.

4.1. Application of Kalman filters for medium- to short-range wind speed forecasts

In the present subsection, the results obtained through the application of a Kalman filter for wind speed prediction, fully analogous to those typically adopted for the correction of surface air temperature, are presented. In this case, a number of forecast horizons are selected and Kalman filtering is applied independently for each forecasting period, with a time step of 24 h. In particular, the considered forecast horizons are 6, 12, 18, 24, 36 h ahead and for each of them the algorithm determines the weights to be applied to the model output as a function of the forecast error in the past 7 days (see Section 3). Different kinds of Kalman filter implementations have been tested, from the classical linear one to a 4th-order polynomial (see Eq. (1)).

The scatter plots of predicted versus observed wind speed at 10 m AGL at the two anemometric stations Casoni di Suvero and Lago di Giacopiane are reported in Fig. 4. The considered forecasting period is 6 h and the adopted Kalman filter is fully linear. In particular, the first row shows model predictions versus measurements, whereas in the second row Kalman filtered with τ = 24 h versus observed wind speeds are plotted. The grey line is the linear regression, while the bisector corresponds to the black line. It can be seen that the improvement in the wind speed prediction is noticeable for both the stations. In particular, the strong underestimation by the model is remarkably reduced, and the highest observed intensity peaks are better reproduced, especially at Casoni di Suvero. It is evident that the effectiveness of the filter in improving model predictions is related to the accuracy of the model itself. Since any Kalman filtering methodology aims at the elimination of systematic errors, if model direct outputs and measurements are even strongly biased, but fairly correlated, the application of the filter leads to relevant forecast improvement. This is the case, in particular, of Casoni di Suvero, where Kalman filtered wind speed values exhibit a better agreement with observations when compared with model predictions. Instead, Kalman filtering provides less significant improvement in the prediction of wind speed at Lago di Giacopiane. Such station, indeed, is more often characterised by sudden variations in wind speed and direction, particularly during lower average intensity conditions, with respect to the other site, because of the very complex orography surrounding the anemometric site, not adequately resolved by the model. As a consequence, the correlation between BOLAM direct outputs and measurements is poorer and the application of the Kalman filter cannot be as successful as for Casoni di Suvero. The algorithm indeed attempts at minimising the bias, but does not succeed completely in catching the temporal evolution of wind speed and reproducing the observed intensity peaks.

The statistical indices for both model direct outputs and Kalman filtered values are reported in Table 2. In both cases the application of Kalman filtering improves the model prediction reducing the mean error considerably to small negative values, therefore suggesting that the main goal of the filter is fulfilled. It is worth noting that the higher the correlation, the stronger the reduction of bias. Furthermore, the reduction of the mean absolute error for the Kalman filtered results ensures that the discrepancy between the two

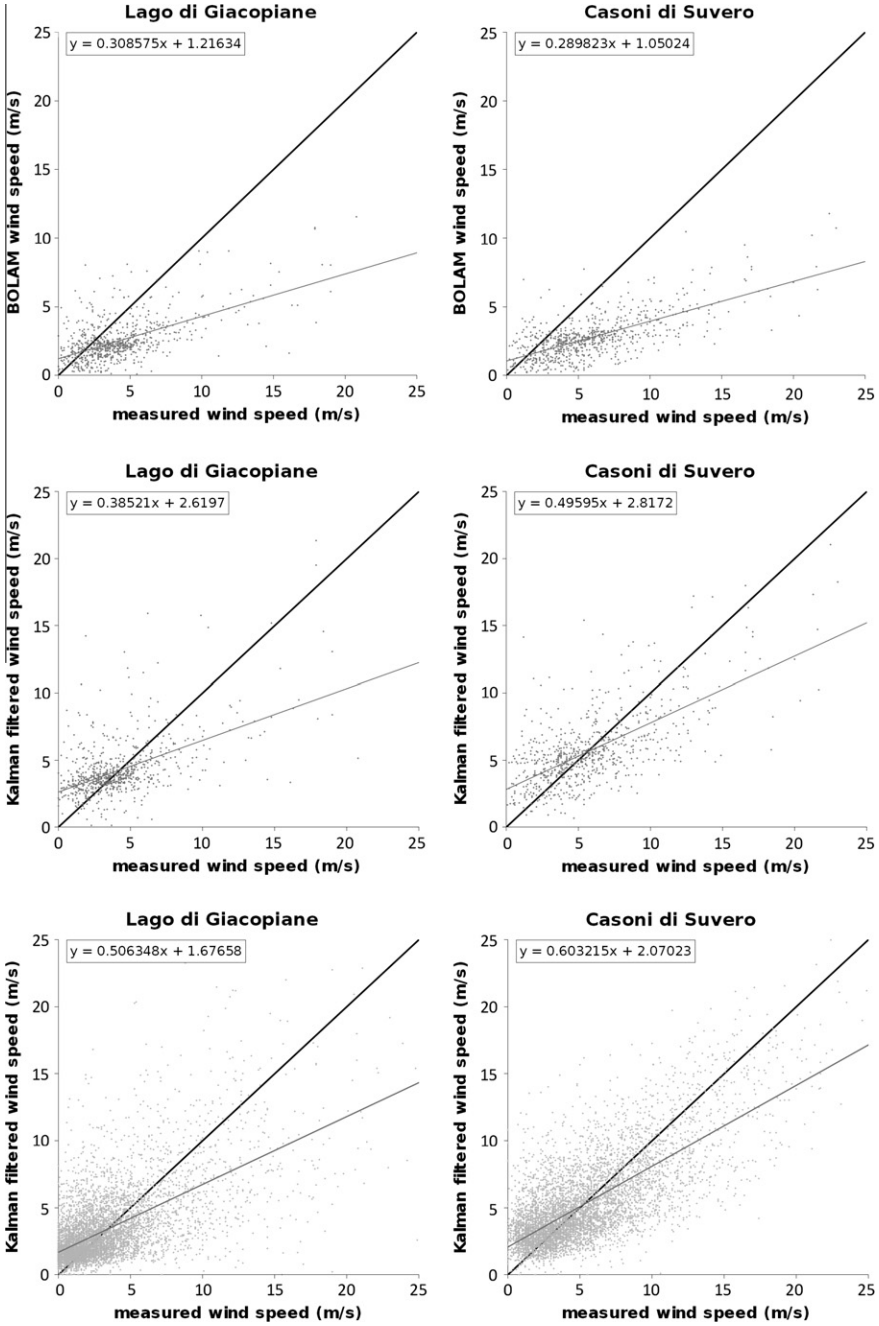

Fig. 4. Model-predicted (first row), Kalman filtered with τ = 24 h (second row), and Kalman filtered with τ = 3 h (third row) 10 m-height wind speeds versus observed values at the two anemometric stations Lago di Giacopiane and Casoni di Suvero (6-h forecasts).

Table 2
Mean error (ME), mean absolute error (MAE) and Pearson correlation coefficient (r) for direct model outputs and Kalman filtered results.

Station and forecasting period	Model			Kalman		
	ME (m/s)	MAE (m/s)	r	ME (m/s)	MAE (m/s)	r
Lago di Giacopiane (+6 h)	−1.77	2.27	0.64	−0.04	1.87	0.57
Casoni di Suvero (+6 h)	−3.11	3.34	0.69	−0.14	2.08	0.66
Casoni di Suvero (+12 h)	−2.56	2.82	0.68	−0.39	2.07	0.68
Casoni di Suvero (+18 h)	−2.63	2.91	0.72	−0.12	2.20	0.68
Casoni di Suvero (+24 h)	−2.59	3.04	0.68	−0.22	2.33	0.65
Casoni di Suvero (+36 h)	−2.63	2.92	0.62	−0.38	2.18	0.63

time series (observed and forecasted) has been decreased despite any possible change in the type of error (underestimation or overestimation). Finally, it can be observed that the application of the filter does not change the correlation coefficient too much,

with a slight worsening at both the stations. This is mainly due to the fact that the Kalman filter does not succeed completely in following the changes of the wind speed and introduces an additional phase shift of the corrected forecast with respect to the measurements. This also contributes to a minor reduction of the mean absolute error with respect to the mean error. Moreover, this kind of methodology has the drawback of a too strong correction for low wind speed values: the algorithm indeed, attempting to minimise the strong negative bias of the model, has the tendency to raise the predicted wind speed, but at low intensities the correction turns out to be excessive. However, this is not a big trouble for applications like wind power forecast, since wind energy converters are inactive below a cut-in threshold of order of 3 m s^{-1}, so that it is much more interesting to have a good prediction of moderate to strong wind situations. Further improvements could be obtained with a site-dependent fine-tuning of the filtering procedure, through the modification of some parameters in the algorithm in order to reduce the variability of the quantity to be filtered and modulate the correction as a function of wind intensity.

To evaluate how the performance of the filter depends on the forecasting period, in Table 2 the statistical indices, calculated for model outputs and Kalman filtered values, are also reported as a function of the forecast horizon. For the sake of brevity, the station of Casoni di Suvero is taken as reference, but analogous considerations are also valid for the other site. It emerges that no evident decay exists in the effectiveness of the correction, but the positive influence of Kalman filtering remains nearly constant with the forecast time, consistently with the results by Galanis et al. [23] and Louka et al. [24].

Finally, the same statistical indices have been calculated for different Kalman filter implementations, from the linear one, discussed insofar, to a 4th-order polynomial (see Eq. (1)). The introduction of non-linearity in the algorithm through polynomial functions did not provide significant improvement, while the plain first order seems to perform even better than higher-order polynomials. Moreover, as the order of the adopted polynomial function increases, also instabilities in the algorithm arise, with no essential contribution in the filter's accuracy, and hence model output improvement.

4.2. Application of Kalman filters for nowcasting purposes

As illustrated in Section 3, the Kalman filter implementation discussed in the previous subsection (corresponding to select a number of forecast horizons and to perform Kalman filtering independently for each forecasting period, with a time step of 24 h) has the drawback of being mainly suitable for the correction of variables characterised by a marked diurnal cycle and a limited inter-daily variability, such as surface air temperature. On the contrary, wind speed is typically much more intermittent and rapidly varying. For this reason, a Kalman filtering procedure, evaluating the weights to be applied to model predictions on the basis of the recent evolution (up to 21 h before) of forecasts and measurements, should provide better results. In particular, model outputs and observations are considered like two continuous time series, regardless of the forecast horizon, and the "time step" τ of the filter corresponds to the maximum frequency at which measurements and forecasts are available (i.e. 3 h in our case). It is clear that this kind of implementation is focused on the very short term, since the estimation of the current state is made taking into account mainly the latest information and a longer forward projection would not make much sense.

The analysis of the temporal evolution of observed, model-predicted and Kalman filtered with τ = 3 h 10 m-height wind speed at the two anemometric stations Lago di Giacopiane and Casoni di Suvero (not shown) suggests that the model forecast is even more

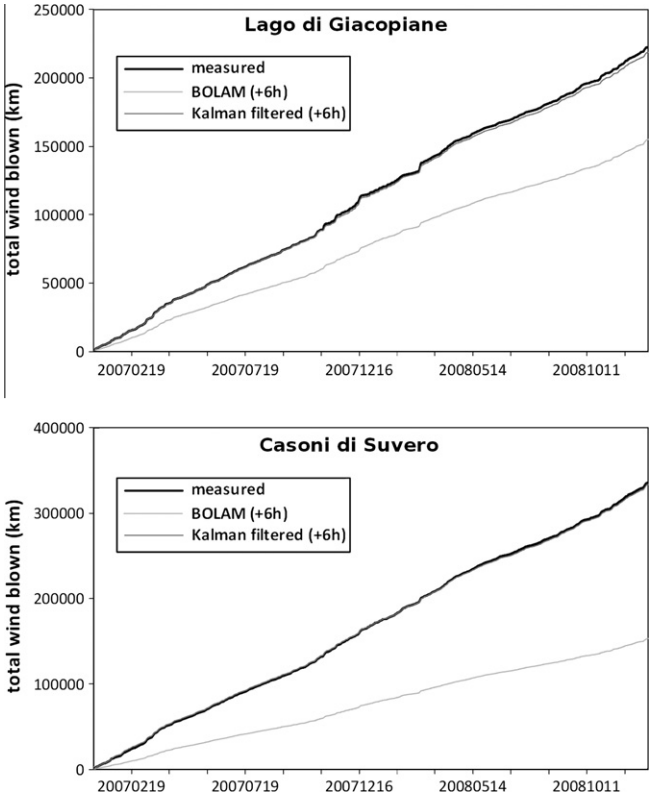

Fig. 5. Total wind blown at Lago di Giacopiane (top) and Casoni di Suvero (bottom), evaluated from observations (black line), model prediction (light grey line) and Kalman filtered values (grey line).

improved with respect to the previous implementation of the filter described in Section 4.1. Indeed, by considering in the calculation recent data only, the model bias should be on average less variable, enhancing the performance of the filter.

The scatter plots for each anemometric station are reported in Fig. 4, third row. Again, very good results are obtained at Casoni di Suvero, with a significant reduction of the underestimating tendency by the model. At Lago di Giacopiane the correction is satisfactory as well, even if a larger dispersion of the data can be observed.

However, the validity of the methodology gets more evident when the total wind blown[2] is analysed. Fig. 5 (top) shows that at Lago di Giacopiane the application of the filter gives satisfactory results, since the corrected wind speeds (grey line) are significantly closer to the measurements (black line) than model predictions (light grey line). It is interesting to observe that the BOLAM model underpredicts systematically the wind speed during all the year. The better performance of the filter at Casoni di Suvero is confirmed by Fig. 5 (bottom): the total wind blown calculated from Kalman-filtered results is essentially coincident with that obtained from measurements, whereas the negative bias of the model is evident again. For this anemometric station, the daily percentage error, defined as the ratio of the absolute difference between the model-predicted and the observed over the observed total wind blown, is on average about 50%. After Kalman filtering, such error drops to 0.3%.

In Table 3 (columns 2–3) the statistical indices summarising the overall performance of the filter are reported and compared with those obtained assuming a time step of 24 h and shown in Table 2. A further reduction of the mean error to almost null values

[2] The total wind blown is defined as the cumulative distance travelled by the wind during a given time.

Table 3
Mean error (ME), mean absolute error (MAE) and Pearson correlation coefficient (r) for different Kalman filter implementations.

Station	Kalman (τ = 24 h), 6-h forecasts			Kalman (τ = 3 h), 6-h forecasts			Kalman (τ = 3 h), 3-h forecasts		
	ME (m/s)	MAE (m/s)	r	ME (m/s)	MAE (m/s)	r	ME (m/s)	MAE (m/s)	r
Lago di Giacopiane	−0.04	1.87	0.57	−0.06	1.92	0.65	−0.05	1.76	0.70
Casoni di Suvero	−0.14	2.08	0.66	−0.04	2.05	0.72	−0.02	1.88	0.77

can be noted at both stations, confirming the validity of the methodology. The mean absolute error lowers and correlation gets stronger, with the exception of Lago di Giacopiane for the 6 h forecast. The last column of Table 3 reports the statistical indices for the shortest forecast term, namely 3 h, showing a further improvement at all sites, as it could be expected. In particular, both ME and MAE are reduced, while the correlation is much higher, with values of 0.7 at Lago di Giacopiane and almost 0.8 at Casoni di Suvero.

These results suggest that this kind of Kalman filtering methodology should be even more effective at a shorter term, of order of 1 h or less. Supposing one to be provided with some kind of model, either physical or statistical, capable to make wind speed predictions at such high temporal resolution, and also with measurements at the same rate, the implementation of a Kalman filter to adjust the model forecast is in principle expected to give a significant contribution for several applications, such as, for instance, short-term power prediction in a wind farm.

5. Wind power prediction by means of NWP model output corrected through Kalman filtering

In the present section, the wind speed measurements available at the international standard reference height of 10 m AGL at the two anemometric stations Casoni di Suvero and Lago di Giacopiane together with the output of the NWP model BOLAM have been used to estimate the daily-averaged wind speed and the daily wind energy production of the two NEG MICON 750/48 wind turbines of the wind farm at Varese Ligure. The procedure adopted to calculate wind speed and wind energy at the wind farm site from the wind speed measured and simulated at the anemometric stations is described in the following subsections.

5.1. Calculation of daily-averaged wind speeds at the wind farm site

The wind speed measurements at the two aforementioned anemometric stations, $V^i\big|_{mast}$ (where $i = 1,2$ refers to the position (x_i, y_i) of Casoni di Suvero or Lago di Giacopiane), were available with a sampling rate of 10 min for a total number of 144 observations every 24 h, whereas the output of the BOLAM simulations at the same locations, $V^i\big|_{NWP}$, were stored every 3 h, namely eight values every day at 00, 03, 06, 09, 12, 15, 18, 21 UTC.

Following the procedure explained in Section 4.2, the two time series $V^i\big|_{NWP}$ have been processed for the whole period of availability (2 years from the 1st of January 2007 to the 31st of December 2008) through a Kalman filter with $\tau = 3$ h to obtain two new time series based on a forecast horizon of +3 h. In other words, the difference between measured and simulated wind speeds at the two anemometric stations for every concurrent time-step t, $\Delta V^i_t = V^i_t\big|_{mast} - V^i_t\big|_{NWP}$, is used to estimate the corrections ΔV^i_{t+1} valid for the next time-step $t + 1$, i.e. 3 h ahead. It is worth noting that this procedure is equivalent to applying a nowcasting process to $V^i_t\big|_{NWP}$ in order to perform a very-short term forecast of the wind speed at the two anemometric stations. A new value of the forecast correction ΔV^j_{t+1} valid at the wind farm site (x_j, y_j) is then calculated trough an interpolation algorithm based on the inverse distance from the two anemometric stations to the second power, and added to the BOLAM simulation output in order to obtain an estimate of the wind speed at the wind farm site $V^j_{t+1} = V^j_{t+1}\big|_{NWP} + \Delta V^j_{t+1}$. In the present paper, only one position (x_j, y_j) in between the two NEG MICON 750/48 wind turbines has been considered representative of the whole wind farm site because the wind turbines are very close each other (approximately 100 m) with respect to the grid spacing of the BOLAM model (approximately 7 km). Indeed, due to the low resolution of the model, the value of V^j_{t+1} calculated at the position of the wind turbines does not change considerably.

The obtained values of V^j_{t+1} still refer to the standard height of 10 m AGL, so that they have to be converted to the corresponding wind speed values at the height of 50 m AGL, i.e. the hub height of the NEG MICON 750/48 wind turbines. This conversion has been performed assuming the wind profile to follow a standard power law, which is a very simple procedure that does not take into account the dependence of the profile on the local topographical effects, roughness changes, and atmospheric stability. It is worth noting, however, that the systematic errors of a NWP model at 10 m AGL might be also different from the corresponding systematic errors at 50 m AGL for some reasons. The shape of the lower part of the vertical wind profiles simulated by a numerical model depends strongly on the surface layer (SL) scheme and the planetary boundary layer (PBL) similarity theory used in the model formulation.[3] On one hand, the SL scheme uses different kinds of atmospheric information like the radiative forcing from the radiative scheme and the precipitation forcing from the microphysics and convective scheme to provide the vertical fluxes of heat, momentum, and moisture at the terrain surface, which, in turn, have a strong impact on that part of the wind profiles closer to the surface, i.e. in the SL. On the other hand, the parameterisation of the vertical mixing due to the sub-grid scale turbulence, which is usually evaluated in the PBL scheme through an effective eddy diffusion coefficient, is responsible for the eddy transport of heat, momentum, and moisture within the whole PBL, therefore influencing the shape of the vertical wind profiles also in the SL. Finally, depending on the atmospheric stability, more or less pronounced speed-up or speed-down effects can occur in the SL over complex topography, further modifying the shape of the wind profiles closer to the surface. These considerations suggest that the systematic error at 50 m AGL could, in general, be different to the error at 10 m AGL and possibly slightly lower as the wind is less influenced by those parameters that have a very local influence and do not change during the computation, e.g. the roughness length. Unfortunately, the wind fields stored in the BOLAM database, used in the present study, are available at 10 m AGL and at the geopotential heights corresponding to the pressure surfaces commonly used for meteorological purposes, namely 1000, 925, 850 hPa, etc., which correspond to average geopotential heights of about 0, 750, 1500 m AGL, respectively. Since the elevation above sea level of the two anemometric stations of Lago di Gia-

[3] The order of magnitude of the PBL height is $h \approx 1000$ m. The height of the SL is commonly assumed equal to $0.1h$ from the terrain surface.

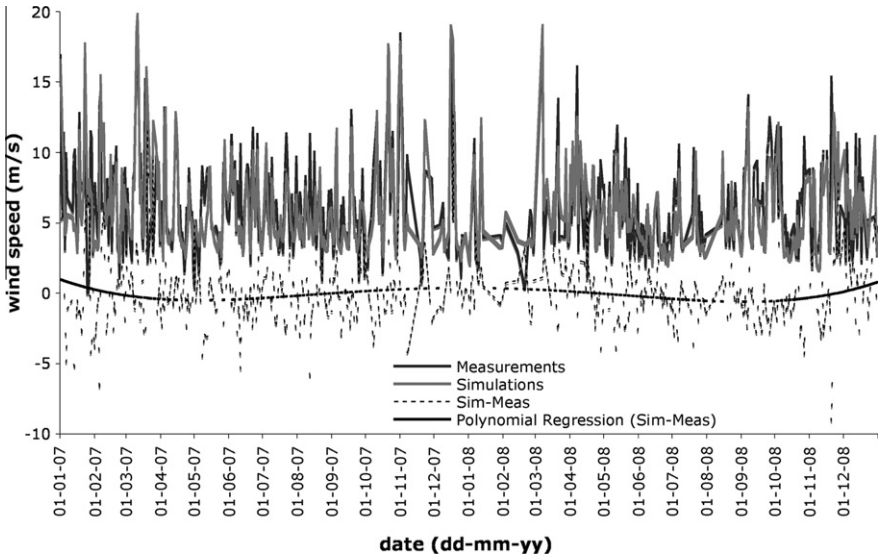

Fig. 6. Time series of simulated (BOLAM output corrected by means of Kalman filtering) and measured daily-averaged wind speeds at the wind farm of Varese Ligure. The difference between simulated and measured values is also shown, as well as its regression with a polynomial function of fourth order.

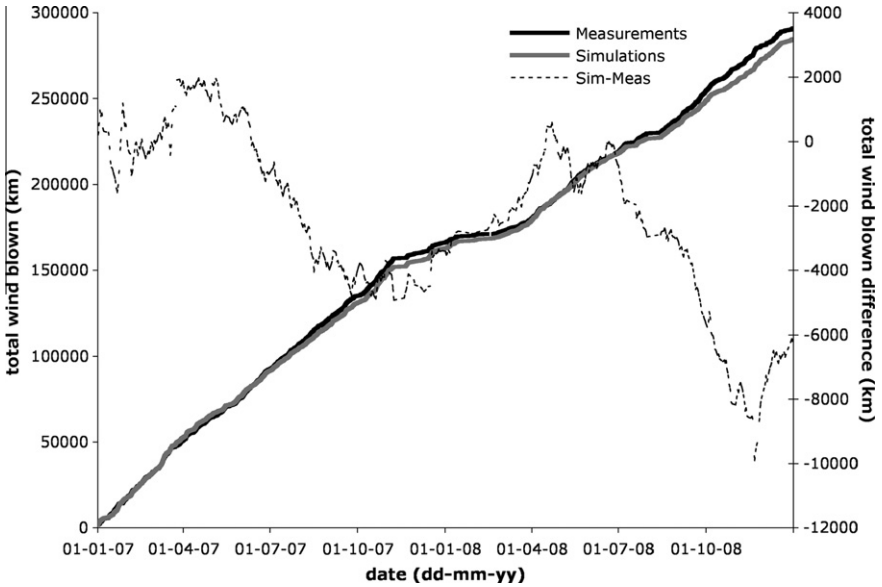

Fig. 7. Total wind blown evaluated at the wind farm of Varese Ligure: simulations (light grey line), measurements (black line), and difference between simulations and measurements (dotted black line in the secondary *y*-axis).

copiane and Casoni di Suvero is around 1000 m (see Table 1), this means that the wind speed at 50 m AGL should be interpolated between the wind speed at 10 m AGL and the wind speed at the pressure surface of 850 hPa, which is more or less at 500 m AGL. In this case, the variability induced in the SL by the physical factors mentioned above would be almost completely masked by the interpolation procedure as the two points are too far each other.

In the authors' opinion, this drawback is not very important in this context since the present paper is focused on presenting a methodology rather than on obtaining accurate evaluations of the considered variables. For practical purposes, however, it is recommended to adopt a procedure as more reliable and realistic as possible.

Finally, for each day the corresponding eight values of the wind speed at 50 m AGL forecasted at the wind farm site are averaged in order to obtain an estimate of the daily-averaged wind speeds at the NEG MICON 750/48 hub height. Fig. 6 shows the comparison between simulated (solid dark grey line) and measured[4] (solid light grey line) values of daily-averaged wind speed at the wind farm of Varese Ligure, as well as their difference (dashed black line). Apart from random fluctuations, which are characterised by a standard deviation of the differences of 2.4 m/s, the simulated daily-averaged wind speeds follow quite well the measurements, at least from a qualitatively point of view. The solid black line, which represents the polynomial regression of fourth order of the wind speed differences, shows that the simulated values are, on average, slightly higher during late winter and early spring and lower the rest of the year. This is also evident in Fig. 7, which shows the total wind blown, de-

[4] This is actually the mean value of the measured daily-averaged wind speeds of the two wind turbines. It is indicated only as "measured daily-averaged wind speed" for the sake of simplicity.

fined as the cumulative distance (km) travelled by the wind during a given time, calculated at the wind farm site with simulated and measured data, and their difference. The latter, in particular, highlights the different trends during colder and warmer seasons.

This behaviour is probably due to the intrinsic nature of the correction applied by the Kalman filter to the original BOLAM simulations. In fact, the filter produces the final value of these corrections accounting for a long-term (i.e. seasonal) and a short-term (i.e. daily) bias of the Numerical Weather Prediction model with respect to measurements. The Liguria region is characterised by very different wind regimes during summer and winter, with prevailing lower wind speeds during the warm season and much higher wind speeds during the cold season [48,49]. When the season changes, the wind regimes change rather abruptly, but the seasonal bias of the filter still remains larger or smaller with respect to the current situation, because the time that the filter requires to adapt to the new wind conditions is greater than the seasonal change. After the first and second year, however, the percentage error, defined as the ratio of the absolute difference between simulated and measured winds blown at the wind farm site over the measured one, is 2.1% and 2.2%, respectively. In principle, the percentage error should be dependent on the particular time window and on the length of the period of time taken into account. The fact that after one or 2 years it almost does not change and that the light grey line (simulations) runs after the black line (measurements) in Fig. 6, seems to suggest that the filter, even if with some delay, is successful in keeping the bias of the total wind blown limited.

5.2. Calculation of the daily wind energy production of the NEG MICON 750/48 wind turbines

After that the time series (eight values per day for a 2-year period) of the wind speed at the hub height at the wind farm site has been calculated (see previous section), this has been converted into

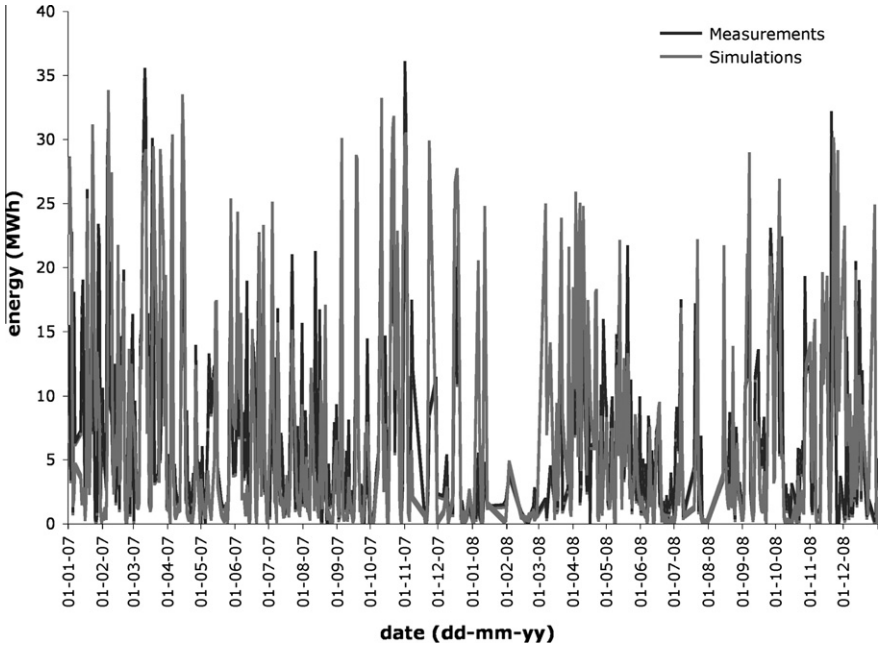

Fig. 8. Time series of calculated and measured daily-cumulated wind energy produced by the two NEG MICON 750/48 wind turbines at the wind farm of Varese Li-gure.

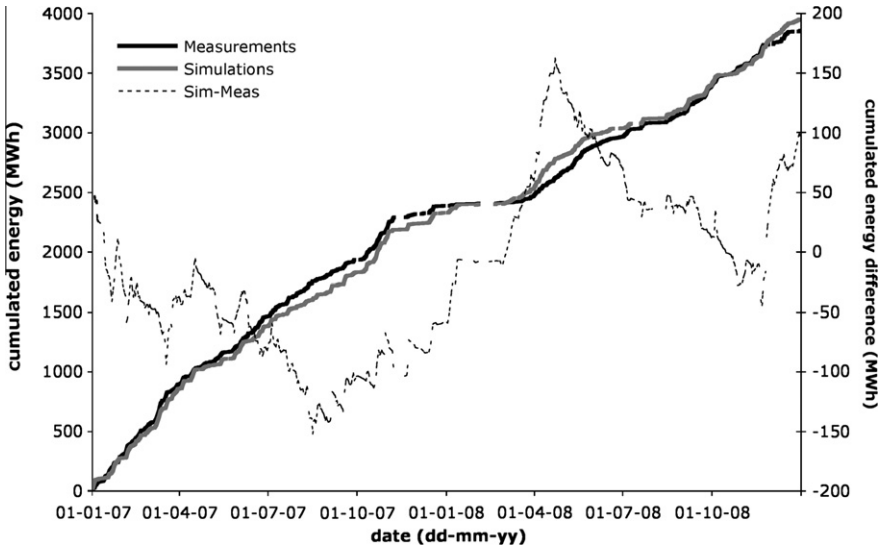

Fig. 9. Cumulated energy corresponding to the production of two NEG MICON 750/48 at the wind farm of Varese Ligure: simulations (light grey line), measurements (black line), and difference between simulations and measurements (dotted black line in the secondary *y*-axis).

the corresponding time series of the wind power produced by a NEG MICON 750/48 by means of its theoretical power curve delivered by the manufacturer. Then, the time series of wind power has been converted into energy output multiplying each value by the discrete time interval $\Delta t = 3$ h, according to the sampling time of the wind speed data set. The transformation from power to energy is rather rough because each wind speed value is assumed to remain constant for the entire time interval, but a certain level of approximation is unavoidable as no information is available about the real behaviour of the wind between two subsequent wind speed values. In case of practical applications, a better estimation of the true wind energy output could be achieved, for instance, using different settings for the output saving time in the NWP model control files, i.e. a higher frequency, as well as using a linear or polynomial fit among the discrete values of the wind speed time series instead of assuming a step function like in the present case.

The consistency of the transformation from wind speeds at 50 m AGL to wind energy output values has been evaluated through the comparison between calculated and actually produced daily-cumulated wind energy of the two NEG MICON 750/48 wind turbines, shown in Fig. 8. Analogously to the behaviour presented in Fig. 6 and discussed in the previous Section 5.1, on average there exists a pretty good agreement between calculated and measured values both for low and high energies. The cumulated energy output for calculated and measured data and their difference is plotted in Fig. 9. As expected, the difference between calculated and measured data, which represents the trend of the filter to correct the bias of the simulations, is again very similar to the one showed for wind speed, with decreasing (increasing) behaviour during the warm (cold) season (apart from the initial period that is not really representative as the filter is still collecting the training set to tune its parameters). After the first and second year the percentage error, defined as for the wind speed, is 2.5% and 2.4%, respectively.

6. Conclusions

In the present paper, a Kalman filtering procedure for the local adjustment of numerical wind speed predictions for wind energy purposes has been proposed. In particular, the methodology has been applied, in a hindcast mode, to a 2-year-long data set, consisting of both gridded forecast fields provided by the mesoscale NWP model BOLAM, with a horizontal resolution of about 7 km, and wind speed recordings at 10 m AGL from two anemometric stations located in the Ligurian territory. The procedure has been tested with wind speed and wind energy output data from a wind farm located in between the two anemometric stations.

The results have shown that this methodology is capable to provide significant forecast improvement with respect to model direct outputs, leading to the elimination of systematic errors. The forecast skill has been proven to be site-dependent. Best results are obtained at sites where measurements and model predictions exhibit a higher correlation, even if with a large bias, like at Casoni di Suvero (see Fig. 5). On the contrary, for anemometric stations located in complex topography areas leading to irregular anemological regimes that cannot be properly described by the model due to its too coarse resolution, Kalman filtering is less effective, though important improvements can be obtained as well, like at Lago di Giacopiane.

Depending on the kind of Kalman filter implementation and on the available modelling system, possible applications range from nowcasting (up to a few hours) to medium-range forecasts (a few days). Beyond the traditional meteorological use, this technique may find several applications in the engineering sector. In particular, in the present paper it is shown that this procedure can be used to provide improved input to a wind power forecast model with respect to NWP direct outputs. The results obtained for the wind farm of Varese Ligure have proven that the procedure is very promising also for wind farms located in complex terrain. Moreover, a site-dependent fine-tuning of the filtering procedure, through the modification of some parameters in the algorithm in order to reduce the variability of the quantity to be filtered and modulate the correction as a function of wind intensity, can provide further benefits.

The computing time required by the whole procedure is extremely limited, of order of a few minutes. Therefore, this work suggests that the use of very expensive computational facilities to perform high-resolution (<6 km) applications for wind energy predictions might be avoided by the combined use of moderate-resolution NWP models and an adaptive statistical technique such as Kalman filtering, providing similar or even more accurate predictions at wind farm scale. Only in very complex situations or in areas where thermal circulations prevail over synoptic flows, the implementation of higher resolution models could be required as the random behaviour of the thermally-driven flows still cannot be represented fully satisfactorily by coarse-grid meteorological models. In the situations when synoptic flows prevail, on the contrary, NWP models are supposed to perform well in catching the temporal evolution of wind speed and Kalman filtering should guarantee the elimination of most of the bias. In an operational setting, this might lead to improvements in electricity market bidding strategies as well as allow better maintenance scheduling. Such improvements can greatly ease wind power integration into conventional systems, thus favouring an increase in the use of wind as a renewable energy source.

Acknowledgements

The authors are grateful to Mrs Brigida Melga for her support in the implementation of Kalman filtering procedures. The Ligurian Environmental Protection Regional Agency (ARPAL), and Dr. Elisabetta Trovatore and Dr. Fabiana Castino in particular, are gratefully acknowledged for providing the anemometric data from the regional observing network. The authors warmly acknowledge ACAM Company for providing us with anemometric and energy production data of the wind farm at Varese Ligure.

References

[1] Giebel G, Brownsword R, Kariniotakis G, Denhard M, Draxl C. The state-of-the-art in short-term prediction of wind power a literature overview, 2nd ed. Project report for the Anemos.plus and SafeWind projects, Risø, Roskilde, Denmark; 2011. 109 pp.
[2] Bossanyi EA. Short-term wind prediction using Kalman filters. Wind Eng 1985;9:1–8.
[3] Vihriälä H, Ridanpää P, Perälä R, Söderlund L. Control of a variable speed wind turbine with feedforward of aerodynamic torque. In: Proc of the European wind energy conf. Nice, France: European Wind Energy Association; 1999. p. 881–84.
[4] Dutton AG, Kariniotakis G, Halliday JA, Nogaret E. Load and wind power forecasting methods for the optimal management of isolated power systems with high wind penetration. Wind Eng 1999;23:69–87.
[5] Fukuda H, Tamaki S, Nakamura M, Nagai H, Shijo F, Asato S, et al. The development of a wind velocity prediction method based on a data-mining type auto-regressive model. In: Proc of the European wind energy conf. Copenhagen, Denmark; 2001, p. 741–44.
[6] Alexiadis MC, Dokopoulos PS, Sahsamanoglou HS, Manousaridis IM. Short-term forecasting of wind speed and related electrical power. Sol Energy 1998;63:61–8.
[7] Bechrakis DA, Sparis PD. Wind speed prediction using artificial neural networks. Wind Eng 1998;22:287–95.
[8] Sfetsos A. A novel approach for the forecasting of mean hourly wind speed time series. Renew Energy 2001;27:163–74.
[9] Chèruy F, Speranza A, Sutera A, Tartaglione N. Surface winds in the Euro-Mediterranean area: the real resolution of numerical grids. Ann Geophys 2004;22:4043–8.

[10] Accadia C, Zecchetto S, Lavagnini A, Speranza A. Comparison of 10-m wind forecasts from a regional area model and QuikSCAT scatterometer wind observations over the Mediterranean Sea. Mon Wea Rev 2007;135: 1945–60.
[11] Mass CF, Ovens D, Westrick K, Colle BA. Does increasing horizontal resolution produce more skillful forecasts? Bull Am Meteor Soc 2002;83:407–30.
[12] Glahn HR, Lowry DA. The use of model output statistics (MOS) in objective weather forecasting. J Appl Meteor 1972;11:1203–11.
[13] Müller MD. Effects of model resolution and statistical postprocessing on shelter temperature and wind forecasts. J Appl Meteor Climatol 2011;50:1627–36.
[14] Hart KA, Steenburgh WJ, Onton DJ, Siffert AJ. An evaluation of mesoscale-model-based model output statistics (MOS) during the 2002 Olympic and Paralympic Winter Games. Wea Forecast 2004;19:200–18.
[15] Landberg L. Short-term predictions of local wind conditions. Ph.D. thesis. Risoe National Laboratory, Denmark; 1994.
[16] Joensen A, Giebel G, Landberg L, Madsen H, Nielsen H. Model output statistics applied to wind power prediction. In: Proc of the European wind energy conf. Nice, France: European Wind Energy Association; 1999, p. 1177–80.
[17] Cheng WYY, Steenburgh WJ. Strengths and weaknesses of MOS, running-mean bias removal, and Kalman filter techniques for improving model forecasts over the Western United States. Wea Forecast 2007;22:1304–18.
[18] Brown RG, Hwang PYC. Introduction to random signals and applied Kalman filtering. 2nd ed. John Wiley and Sons; 1992.
[19] Persson A. Kalman filtering a new approach to adaptive statistical interpretation of numerical meteorological forecasts. ECMWF Newslett 1990;46:16–20.
[20] Dragulanescu L. Application des filtres Kalman pour ajuster les temperatures prognosées avec un modèle numérique. Meteor. Hydrol. 1993;23:11–4 [in French].
[21] Kalnay E. Atmospheric modeling, data assimilation and predictability. Cambridge University Press; 2002.
[22] Galanis G, Anadranistakis M. A one dimensional Kalman filter for the correction of near surface temperature forecasts. Meteor Appl 2002;9: 437–41.
[23] Galanis G, Louka P, Katsafados P, Pytharoulis I, Kallos G. Applications of Kalman filters based on non-linear functions to numerical weather predictions. Ann Geophys 2006;24:2451–60.
[24] Louka P, Galanis G, Siebert N, Kariniotakis G, Katsafados P, Pytharoulis I, et al. Improvements in wind speed forecasts for wind power prediction purposes using Kalman filtering. J Wind Eng Ind Aerodyn 2008;96:2348–62.
[25] Roeger C, Stull R, McClung D, Hacker J, Deng X, Modzelewski H. Verification of mesoscale numerical weather forecasts in mountainous terrain for application to avalanche prediction. Wea Forecast 2003;18:1140–60.
[26] Anadranistakis M, Lagouvardos K, Kotroni V, Skouras K. Combination of Kalman filter and an empirical method for the correction of near-surface temperature forecasts: application over Greece. Geophys Res Lett 2002;29:1776–9.
[27] Anadranistakis M, Lagouvardos K, Kotroni V, Elefteriadis H. Correcting temperature and humidity forecasts using kalman filtering: potential for agricultural protection in Northern Greece. Atmos Res 2004;71:115–25.
[28] Kariniotakis G, Coauthors. Next generation short-term forecasting of wind power – overview of the ANEMOS project. In: Proc of EWEC 06. Athens, Greece: European Wind Energy Association; 2006.
[29] Buzzi A, Fantini M, Malguzzi P, Nerozzi F. Validation of a limited area model in cases of Mediterranean cyclogenesis: surface fields and precipitation scores. Meteor Atmos Phys 1994;53:137–53.
[30] Buzzi A, Malguzzi P. The BOLAM III model: recent improvements and results. MAP Newslett 1997;7:98–9.
[31] Lagouvardos K, Kotroni V, Koussis A, Feidas C, Buzzi A, Malguzzi P. The meteorological model BOLAM at the National Observatory of Athens: assessment of two-year operational use. J Appl Meteor 2003;42:1667–78.
[32] Buzzi A, Foschini L. Mesoscale meteorological features associated with heavy precipitation in the southern Alpine region. Meteor Atmos Phys 2000;72: 131–46.
[33] Corazza M, Buzzi A, Sacchetti D, Trovatore E, Ratto CF. Simulating extreme precipitation with a mesoscale forecast model. Meteor Atmos Phys 2003;83:131–43.
[34] Buzzi A, Tartaglione N, Malguzzi P. Numerical simulations of the 1994 Piedmont flood: role of orography and moist processes. Mon Wea Rev 1998;126:2369–83.
[35] Buzzi A, D'Isidoro M, Davolio S. A case-study of an orographic cyclone south of the Alps during the MAP SOP. Quart J Roy Meteor Soc 2003;129:1795–818.
[36] Richard E, Cosma S, Benoit R, Binder P, Buzzi A, Kaufmann P. Intercomparison of mesoscale meteorological models for precipitation forecasting. Hydrol Earth Syst Sci 2003;7:799–811.
[37] Lagouvardos K, Floros E, Kotroni V. A grid-enabled regional-scale ensemble forecasting system in the Mediterranean Area. J Grid Comput 2010;8:181–97.
[38] Kalman RE. A new approach to linear filtering and prediction problems. Trans ASME 1960;82:35–45.
[39] Kalman RE, Bucy RS. New results in linear filtering and prediction problems. Trans ASME 1961;83:95–108.
[40] Gelb A. Applied optimal estimation. MIT Press; 1974.
[41] Maybeck PS. Stochastic models, estimation, and control, vol. 1. Academic Press; 1979.
[42] Lewis FL. Optimal estimation: with an introduction to stochastic control theory. John Wiley and Sons; 1986.
[43] Jacobs OLR. Introduction to control theory. 2nd ed. Oxford University Press; 1993.
[45] Crochet P. Adaptive Kalman filtering of 2-metre temperature and 10-metre wind-speed forecasts in Iceland. Meteor Appl 2004;11:173–87.
[46] Giebel G. On the benefits of distributed generation of wind energy in Europe. Ph.D. thesis, Carl von Ossietzky Universitat Oldenburg, Dusseldorf, Germany; 2001.
[47] Wilks DJ. Statistical methods in the atmospheric sciences: an introduction. 2nd ed. Academic Press; 2006.
[48] Burlando M. The synoptic-scale surface wind climate regimes of the Mediterranean Sea according to the cluster analysis of ERA-40 wind fields. Theor Appl Climatol 2009;96:69–83.
[49] Burlando M, Antonelli M, Ratto CF. Mesoscale wind climate analysis: identification of anemological regions and wind regimes. Int J Climatol 2008;28:629–41.